JGR Oceans

RESEARCH ARTICLE
10.1029/2020JC016282

Key Points:
- A new low PV water mass with large subduction rate is found near equatorial North Pacific and is named as NELPVW
- Under global warming, only NELPVW has a significant increasing trend among all North Pacific low PV water masses
- The equatorial SOT anomaly in the strong NELPVW (EMW) subduction years is completely opposite to those weak subduction years

Supporting Information:
- Supporting Information S1

Correspondence to:
H.-B. Hu
huhaibo@nju.edu.cn

Citation:
Wang, Z., Wen, Z., Hu, H., Song, Z., & Liu, G. (2020). The characteristics of near-equatorial North Pacific low PV water and its possible influences on the equatorial subsurface ocean. *Journal of Geophysical Research: Oceans*, *125*, e2020JC016282. https://doi.org/10.1029/2020JC016282

Received 26 MAR 2020
Accepted 30 JUL 2020
Accepted article online 3 AUG 2020

The Characteristics of Near-Equatorial North Pacific Low PV Water and Its Possible Influences on the Equatorial Subsurface Ocean

Ziyi Wang[1], Zhibin Wen[1,2], Haibo Hu[1,3], Zhenya Song[2], and Guoqiang Liu[4]

[1]CMA-NJU Joint Laboratory for Climate Prediction Studies, Instituted for Climate and Global Change Research, School of Atmospheric Science, Nanjing University, Nanjing, China, [2]First Institute of Oceanography, Ministry of Natural Resources, Qingdao, China, [3]KLME and CIC-FEMD, Nanjing University of Information Science and Technology, Nanjing, China, [4]Bedford Institute of Oceanography, Fisheries and Oceans Canada, Dartmouth, Nova Scotia, Canada

Abstract Using SODA oceanic reanalysis data, the subduction rate and low potential vorticity (PV) water masses in the North Pacific are investigated from January 1870 to December 2008. A new low PV water mass with a large subduction rate is found near-equatorial North Pacific, which is named as the near-equatorial North Pacific low PV water mass (NELPVW), and it is the only one low PV water mass in North Pacific that appears an increasing trend under global warming. Among all the low PV water masses in North Pacific, only Eastern Subtropical Mode Water (EMW) and NELPVW can migrate to the equatorial Pacific and effect subsurface oceanic temperature (SOT) there. Further research shows that the subducted low PV water mass in EMW generation region can migrate to equatorial Pacific through two transport paths, which are called the Western-EMW path and the Central-EMW path. The analysis of Lagrange tracking shows that EMW can migrate and bring SOT anomaly to equatorial Pacific along these paths in 7 years and lead to the almost precisely opposite distributions of equatorial Pacific SOT anomaly between the strong and weak EMW subduction years, while it takes the newly discovered NELPVW less than 3 years to reach the equatorial Pacific along the Western-NELPVW path or the Eastern-NELPVW path after subduction. The distributions of equatorial Pacific SOT anomaly in the strong and weak NELPVW subduction years are approximately reverse too. The actual distribution of the equatorial Pacific SOT is affected by these two low PV water masses at the same time.

Plain Language Summary By calculating annual subduction rate in the North Pacific using SODA oceanic reanalysis data, a new low PV water mass with a large subduction rate is found near equatorial North Pacific, which is named as the near-equatorial North Pacific low PV water mass (NELPVW), and it is the only one low PV water mass with an increasing trend under global warming in North Pacific. The equatorward-transport paths of EMW and NELPVW and consequent impacts on the equatorial SOT are revealed. In the strong EMW subduction years, the SOT anomaly in equatorial Pacific is positive in the east and negative in the west. In the strong NELPVW subduction years, the SOT anomaly of equatorial Pacific is negative in the center and positive in the east and west. The equatorial SOT anomaly in the strong NELPVW (EMW) subduction years is completely opposite to those weak subduction years. This study reveals how the subduction process of the low PV water masses outside the equator affect the distribution of the equatorial Pacific SOT, which is beneficial to the prediction of ENSO in the medium and long term.

1. Introduction

There is a wide range of subsurface water masses characterized by nearly vertically homogeneous temperature and salinity distributions with low PV, which are called the subsurface low PV water mass or mode water (Hanawa & Talley, 2001; Hu et al., 2006; McCartney & Talley, 1982; Worthington, 1959). After subducting into the subsurface layer (viz., subduction), the low PV water mass, which is isolated from the surrounding, moves along the isopycnal and diffuses to other areas and brings the atmospheric forcing signals into the subsurface ocean. The generation and dissipation of the low PV water mass affect various ocean-atmosphere dynamic and thermodynamic processes on a wide range of time scales, which is one of the most important research directions of climate change. The concept of subduction that water was pumped into the Ekman layer in late winter and transported along the isopycnal was first proposed by Iselin (1939). However, the volume of low PV water mass passing through the mixed layer is proved greater than that pumped by Ekman pumping. This issue is unresolved until Stommel (1979) analyzed the oceanic subduction process by the mixed layer depth (MLD) seasonal variation diagnostic scheme. Furthermore, it is believed that the mesoscale oceanic eddies play an important role in North Pacific subtropical mode water (STMW) variability (Shi et al., 2018; Wen et al., 2020).

As subtropical MLD in North Pacific becomes deeper toward the pole, the contribution of the transport across the mixed layer to the total subduction rate is the same order of magnitude or larger than the contribution of Ekman pumping (Huang & Qiu, 1994; Marshall et al., 1993). Qiu and Huang (1995) then defined the annual mean subduction rate and figured out the long-term mean subduction rate in the North Pacific using the data sets of Levitus. Further research found that the change in the subtropical low PV water mass is not only related to the subduction rate (Qu & Chen, 2009) but also related to the changes in the background oceanic current and ventilation position (Kubokawa & Xie, 2002; Yasuda & Hanawa, 1997). And it is found that the annual subduction rate in North Pacific correlates with the Pacific Decadal Oscillation (PDO) (Guo et al., 2018; Toyama et al., 2015). Moreover, Wu et al. (2020) found that decadal-to-multidecadal variability of the mode water in North Pacific is closely related to the Atlantic Multidecadal Variability (AMV).

Three low PV water masses have been discovered in the North Pacific: the Western Subtropical Mode Water (STMW, Masuzawa, 1969), the Central Mode Water (CMW, Nakamura, 1996; Suga et al., 1997), and the Eastern Mode Water (EMW, Hautala & Roemmich, 1998; Huang & Qiu, 1994). The different formation regions result in the specific thermohaline characteristics and different temporal variabilities of these three low PV water masses (Hu et al., 2006) and lead to different potential effects on climate. The STMW is mostly confined to the subtropical ocean circle in the Northwest Pacific (Liu & Hu, 2007). However, the EMW, unlike the STMW, is proved to be transported by the oceanic subtropical gyre from their formation region to western subtropical areas after entering the permanent thermocline (Oka et al., 2011) and leads to interannual-decadal climate changes (Gu & Philander, 1997; Hanawa, 1987). Moreover, Chen et al. (2010) revealed the opposite trend of subduction rates in the Northeast Pacific and Northwest Pacific by an eddy-resolving ocean general circulation model.

There are also many branches about the climatic effects of low PV water masses. For example, the low PV water mass can also affect the subsurface ocean directly by obduction (Qiu & Huang, 1995). Yu et al. (2015) revealed that the PV anomalies of STMW affect the subsurface oceanic transport in the Luzon Strait by changing the subsurface density structure and the zonal velocity. The results of Kobashi et al. (2006) indicated that the formation of subtropical countercurrent is related to the northwest part of STMW. Besides, the subtropical low PV water mass may pass through the subtropical meridional circulation (Gu & Philander, 1997; Liu & Huang, 2012). The meridional circulation between the Pacific subtropical and tropical regions has been proved to slow down after the 1970s, with increasing the sea surface temperature (SST) over the equatorial Pacific (McPhaden & Zhang, 2002). However, it is unclear what role the subtropical low PV water mass may play in it and what mechanism does the low PV water mass affect the tropical Pacific.

With the improvement of global oceanographic observations, many new discoveries have been made about climate change research in the 20th century. It is found that low PV water masses changed greatly with global warming. The subtropical surface water warming has been consistent with global warming over the past six decades, and the warming of the western boundary current is twice the rate of global warming, while the subtropical low PV water mass warms in the speed of twice the rate of surface air warming (Sugimoto et al., 2017). Coupled climate model simulations predicted that in response to global warming, the densities of the mode waters tended to become lighter, which is due to a more stratified upper ocean and thus a shoaling of the winter mixing depth resulting mainly from a reduction of the ocean-to-atmosphere heat loss over the subtropical region (Lee, 2009; Luo et al., 2009). The full simulated evolution of the North Pacific low PV water and Subtropical Countercurrent (STCC) under global warming shows that the low PV water and STCC first show a sharp weakening trend when the radiative forcing increases but then reverse to a slow strengthening trend of smaller magnitude after the radiative forcing is stabilized because the subsequent warming is greater at the subsurface than at the sea surface, destabilizing the upper ocean and becoming favorable for the low PV water formation (Xu et al., 2013).

In recent decades, more and more central ENSO, including warm pool and Modoki types, have occurred in the tropical surface Pacific (Choi et al., 2011; McPhaden et al., 2011). Meanwhile, the relationship between subsurface and surface oceanic gradually revealed. There are two independent modes (ENSO-Induced-TPDV and ENSO-Like-TPDV) in the subsurface layer of the tropical Pacific Ocean (Choi et al., 2013). However, the formation mechanism and distribution of these two subsurface modes are still unclear. Can any low PV water masses transport to the equatorial Pacific carrying their temperature and salinity anomalies? Where is the transport passage of these kinds of low PV water masses? Can these water masses impact on the equatorial Pacific subsurface oceans? These series of scientific issues are discussed in this article.

This study mainly demonstrates the North Pacific low PV water masses and their nonlocal effects on equatorial subsurface. The data sets and methods used in the article are described in section 2. Characteristics of the newly discovered NELPVW are introduced in section 3. Section 4 shows the influence of the EMW and NELPVW on the SOT of the equatorial Pacific. Section 5 offers summary and discussion.

2. Data and Method

The Simple Ocean Data Assimilation (SODA, Carton et al., 2005, download at http://apdrc.soest.hawaii.edu/datadoc/soda_2.2.4.php) data version 2.2.4 is used in this paper. SODA2.2.4 data rely on Parallel Ocean Program physics ocean model and assimilated ocean observation data over 100 years. The time span is from January 1871 to December 2008 with a monthly mean temporal resolution. The spatial range is nearly complete coverage of the globe with the resolution of $0.5° \times 0.5°$. There are 40 layers in the vertical direction, with the maximum depth over 5,000 m.

To examine the result of subduction rate calculated by the SODA data, the Levitus-94 data (Levitus & Boyer, 1994) are also used. Levitus-94 monthly data are from World Ocean Atlas 1994, which is an atlas of objectively analyzed fields of major ocean parameters. The data set includes fundamental ocean parameters, such as potential density, salinity, temperature, potential temperature, and MLD. The spatial horizontal resolution is $1° \times 1°$. Levitus-94 monthly data used in this study were obtained from the website (http://iridl.ldeo.columbia.edu/SOURCES/.LEVITUS94/.MONTHLY/).

To make the existence of NELPVW more convincing, we add analyses of global ocean Array for Real-time Geostrophic Oceanography (Argo) gridded data set (Barnes objective analysis, BOA_Argo) to compare with the SODA data. The BOA_Argo gridded data set is produced based on refined Barnes successive corrections by adopting flexible response functions based on a series of error analyses to minimize errors induced by nonuniform spatial distribution of Argo observations. The time span is from January 2004 to December 2019 with a monthly mean temporal resolution. The spatial range is nearly a complete coverage of the globe with the resolution of $1° \times 1°$. There are 58 layers in the vertical direction, with the maximum depth over 2,000 dbar (Lu et al., 2020). BOA_Argo gridded data set used in this study was obtained from the website: (ftp://data.argo.org.cn/pub/ARGO/BOA_Argo/).

We define mode water as water mass that with PV less than or equal to $2.5 \times 10^{-10}\ \mathrm{m}^{-1}\ \mathrm{s}^{-1}$, and lying below the ML, the calculation method of PV is as follows:

$\mathrm{PV} = \frac{f\Delta\sigma_\theta}{\Delta_z}$, where the f is the geostrophic parameter, ρ is the average density of seawater, and $\frac{\Delta\sigma_\theta}{\Delta_z}$ is the vertical gradient of potential density (PD). PV value is conserved in adiabatic motion. Therefore, it is a good basis for studying the generation and migration of low PV water mass.

The generation volume of low PV water mass is measured by the annual mean subduction rate (Qiu & Huang, 1995). The calculation formula in Lagrange field is as follows:

$$S_{ann} = -\overline{\left(w_{EK} - \frac{\beta}{f}\int_{-h_m}^{0} v\,dz\right)} + \frac{1}{T}\left(h_{m,1} - h_{m,2}\right),$$

where w_{EK} is the Ekman velocity at the base of the mixed layer, the β term denotes the vertical velocity reduction due to the meridional velocity in the surface layer, f is the geostrophic parameter, and v is the meridional velocity. The overbar denotes an average over the 1-year Lagrange trajectory. h_m is the

MLD of each month; $h_{m,1}$ and $h_{m,2}$ are the MLDs in the first and second March, respectively. The first term on the right side of the equation represents the contribution by vertical motion, which is called the vertical term. The second term on the right side represents the contribution by horizontal motion, which becomes the lateral induction term.

To study the climatic effects of low PV water masses more specifically, Lagrange tracking method is used. Tracing the low PV water mass along the isopycnal can help us clarify its trajectory, transport duration, and the affected regions. Because the low PV water mass is isolated from the surrounding seawater during transport, the characteristics of low PV can be conserved in the transport, which is a good basis for tracing low PV water mass.

Using the multivariate empirical orthogonal function (MV-EOF) method analyses the equatorial Pacific subsurface oceanic temperature (SOT). Compared with the traditional EOF method, MV-EOF can show the seasonal evolution of SOT. The specific method (Wang, 2010) divides SST data into four seasonal variable fields, the spatial points of each variable are i and j, and the time series length is k. Firstly, the variables are standardized, and a new variable field $Y = (Y_{i,j,k})$ is formed by them, where $i = 1, 2, 3, ..., I$; $j = 1, 2, 3, ..., J$; $k = 1, 2, 3, ... K$. Y is decomposed by the MV-EOF, and then each variable is separated from the decomposed eigenvector and multiplied by its mean square deviation.

3. Characteristics of the NELPVW

In previous studies, many researchers calculated the long-term mean subduction rate using geostrophic current data. However, the actual ocean current is much more complex. In this study, we calculate the long-term mean subduction rate in the North Pacific by SODA (Figure 1), which is much closer to the actual current. Three main subduction regions are located in the region of 30–35°N, 145–165°E, the region of 40–44°N, 153–162°E, and the region of 23–30°N, 145–130°W. Comparing with previous researches, new spatial characteristics of the subduction rate are found. The subtropical subduction region is more close to the central subduction region along the Kuroshio Extension, which implies that these two mode water masses are not independent of each other in SODA2.2.4. More importantly, besides the three main subduction regions, the near-equatorial Pacific region (11–20°N, 150°E–180°) with a high subduction rate is found, which has never been discussed in the previous studies. Though the subduction rate value in this region is slightly smaller than the northern region, the spatial range is very large.

In addition, the vertical subduction term accounts for 57.71% of the total annual subduction rate, much larger than other regions, which is much related to the trade wind. The different distribution of subduction rate in this new discovered NELPVW region, compared to that in Qiu and Huang (1995), is mainly caused by using different velocity in the calculation. The change of velocity data affects the vertical term directly by the change of meridional velocity. Moreover, indirectly, it affects the lateral term, which is defined as the difference of MLD between the first and following winter along the water mass trajectory, and the trajectory is related to the oceanic velocity.

In this newly discovered high subduction rate area (11–20°N, 150°E–180°), a new low PV water mass is found, which is named as the near-equatorial low PV water (NELPVW). The distributions of NELPVW, EMW, STMW, and CMW are clearly shown in Figure 2b. The summary of the specific characteristics of four North Pacific low PV water masses in the SODA 2.2.4 data is shown in Table 1. The NELPVW is characterized by nearly vertically homogeneous temperature and salinity distributions, with significant seasonal variation signal as well as others (Figure 2d), while its specific characteristics are different from the other three low PV water masses in the North Pacific. The core PD of NELPVW is less than $23\sigma_\theta$, and the temperature ranges from 20 to 25°C; it is the lightest and warmest of the four low PV water in North Pacific. NELPVW exists in the depth range of 50–120 m (Figure 2c), with a flatter three-dimensional structure, which is the shallowest of the four low PV water in North Pacific. Therefore, it is much easier to influence by atmosphere.

It is worth mentioning that the existence of newly discovered low PV water and its potential impact on equatorial Pacific can be influenced by the choice of data sets to some extent. To make the existence of NELPVW more convincing, we add analyses of Levitus-94 data from year 1900 to 1992 and BOA_Argo data from year 2004 to 2016 to compare with the SODA data (Figure 2a). More details about the different distributions of MLD/ PV in SODA2.2.4, Levitus-94, and BOA_Argo data are provided in supporting information (Figure

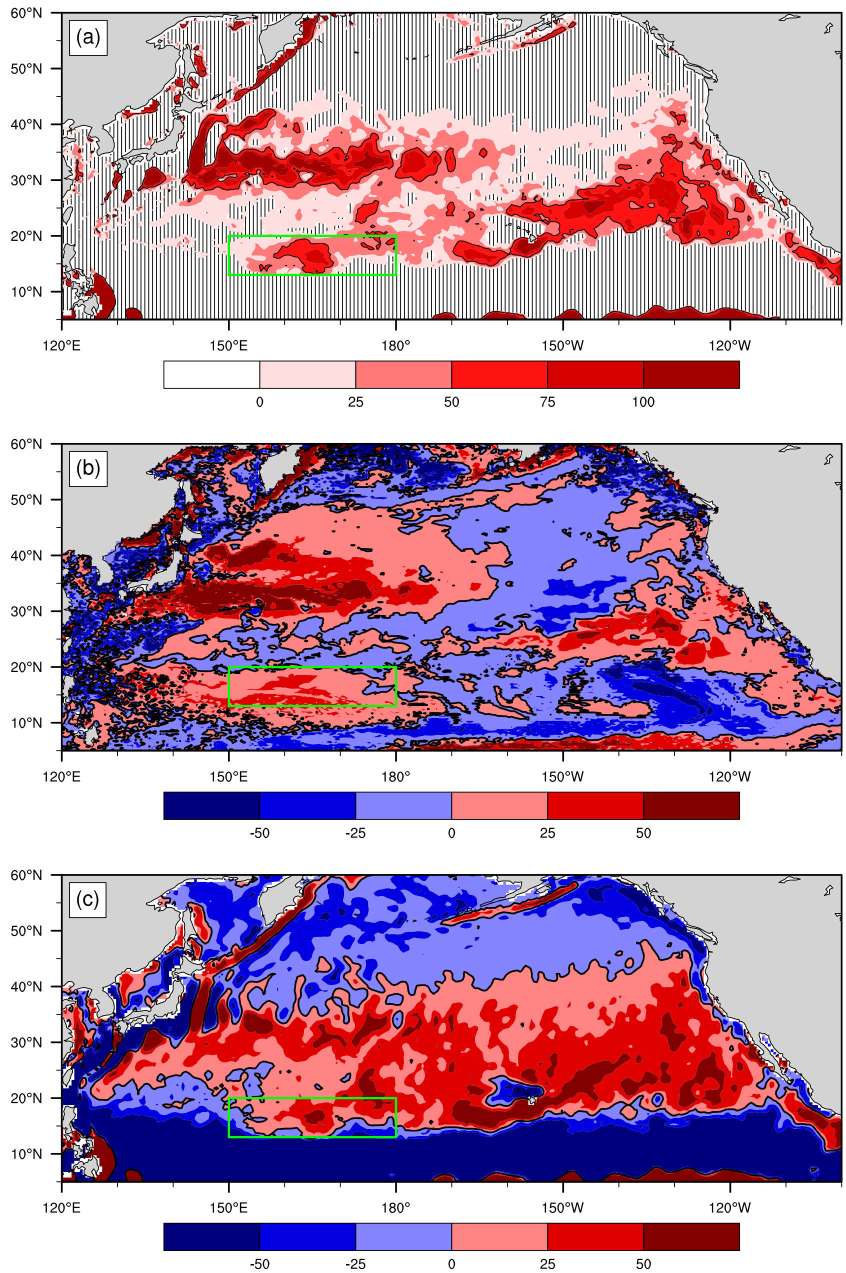

Figure 1. The distributions of long-term mean subduction rate (a), its lateral component (b), and vertical component (c) in North Pacific using SODA 2.2.4 data (shadings; m year^{-1}). The newly discovered region with a large subduction rate is marked by the green frame.

S1/Figure S2). The distribution of long-term mean winter PV and PD in the depth of 90 m with Levitus-94 data and BOA_Argo data in North Pacific is shown in Figure 3. At the depth of 90 m, compared with the SODA data, there is a smaller volume of low PV water mass in the NELPVW generation region analyzed by BOA_Argo data but larger volume analyzed by Levitus-94 data. And compared with the results of SODA data, the core depth of NELPVW is shallower in Levitus-94 data. However, according the annual mean ventilation rate calculated by Qiu and Huang (1995) using Levitus and HR data, the subduction rate in newly discovered NELPVW region is much smaller than the result calculated by SODA data.

The southward horizontal movement can bring near-equatorial water to the region with shallower mixed layer, which causes large lateral term. To exclude the influence of southward western boundary current,

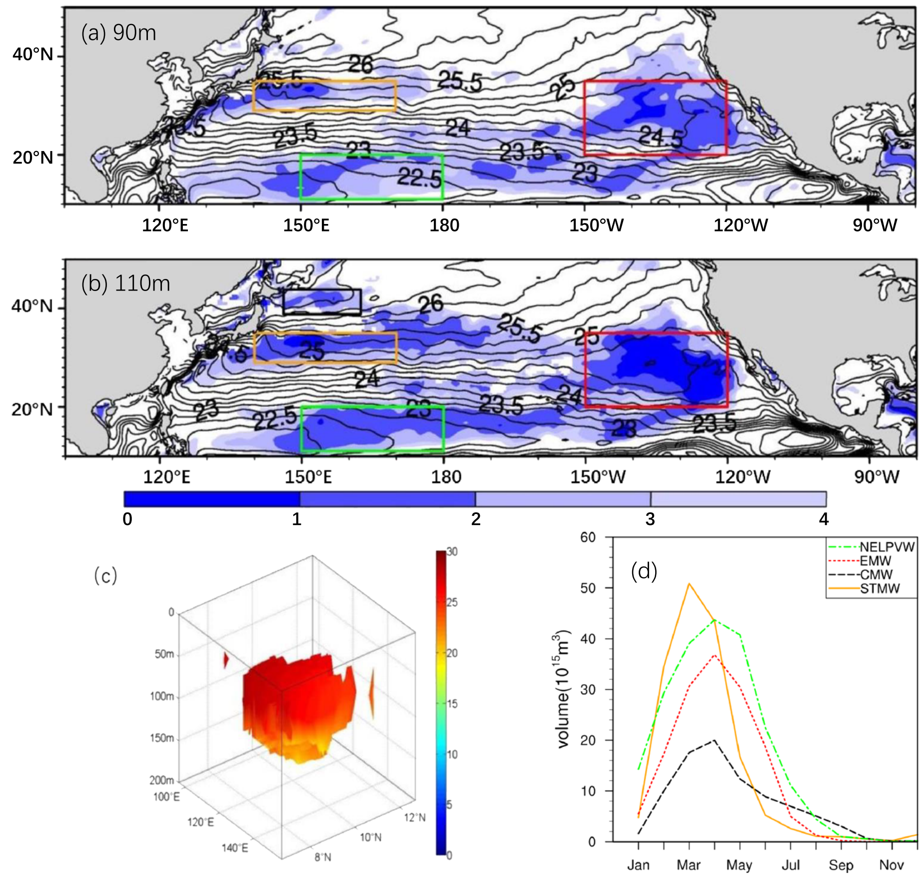

Figure 2. The distributions of long-term mean winter PV (shadings; 10^{-10} m^{-1} s^{-1}) and PD (black contours; kg m^{-3}–1,000) in North Pacific at the depths of 90 m (a) and 110 m (b), green frame represents NELPVW, red frame represents EMW, black frame represents CMW, and orange frame represents STMW. (c) Three-dimensional structure of the long-term mean temperature of NELPVW (shadings; °C). (d) Seasonal variations of the volume of four low PV water masses in the North Pacific, green line represents NELPVW, red line represents EMW, black line represents CMW, and orange line represents STMW.

the subduction rate is calculated using Levitus-94 mixed layer data with different velocities (Figure 4). It is found that the subduction rate value is obvious larger using SODA velocity than the geostrophic and Ekman velocities calculated from the Levitus data. In particular, in the region of 11–20°N and 150–180°E (green frame), high subduction rate almost fills the whole region, and the maximum value there is much larger too.

The geostrophic flow, which is calculated from oceanic density and pressure under the assumption of geostrophic equilibrium, is widely used in the traditional subduction researches (Hu et al., 2006; Qiu & Huang, 1995). To reflect the stirring effect of the atmosphere on the ocean, Ekman velocity is also introduced to this research. However, geostrophic and Ekman flows are only applicable to the inner ocean but not to the lateral boundary region, especially the western boundary current region in the North Pacific. Comparing the long-term mean March geostrophic and Ekman flow fields calculated by Levitus-94 data and the SODA flow fields among the PD layer of 22.6σ_θ (Figure 5), the SODA velocity at the southwest boundary of the North Pacific (marked by green frame in Figure 5) is significantly higher. And it is easier to identify the northward Kuroshio, the southward Mindanao Current, and Equatorial Countercurrent in SODA flow fields. Therefore, comparing to the previous researches, which calculated subduction rate by Levitus-94 data, the subduction rate calculated by SODA data is much closer to the actual situation.

Four subduction rate indexes are obtained by regional mean of the annual subduction rate in generation regions of four low PV water masses, which are defined as the STMW, CMW, EMW, and NELPVW, respectively. The annual subduction rate in the near-equatorial Pacific region is around 75 to 100 m year^{-1}, smaller

Table 1
Characteristics of Four Low PV Water Masses in the North Pacific

Name	Temperature (°C)	Salinity (psu)	Potential density (σ_θ)	Depth range (m)	Vertical item ratio	Area
STMW	12–18	34.1–34.9	25.2–26.2	50–300	5.35%	(30°N–36°N, 140°E–180)
CMW	9–14	33.5–34.5	25.75–26.3	50–200	−15.42%	(40°N–45°N, 145°E–170°E)
EMW	15–21	33.5–34.5	24.5–25	50–120	38.27%	(20°N–35°N, 150°W–120°W)
NELPVW	20–25	34.2–34.7	22.25–23	50–120	57.71%	(11°N–20°N, 150°E–180)

than the other three main subduction regions but still notable (Figure 6). The correlation between each subduction index and the corresponding volume of low PV water mass is significantly positive, which means that the variation of the subduction rate can represent the variation of low PV water mass volume to some extent. STMW had an increasing trend before the 1930s but decreasing after that. STMW and EMW have decadal or interdecadal variations, which are proved in previous research (Hu et al., 2006). Guo et al. (2018) found that the decadal variability of EMW is related to the Pacific Decadal Oscillation (PDO). Moreover, Wu et al. (2020) found that the decadal-to-multidecadal variability of STMW is closely related to the Atlantic Multidecadal Variability (AMV). NELPVW varies significantly on the seasonal, interannual, and interdecadal timescales. For the seasonal variation of NELPVW, the maximum volume appears from March to May but quickly dissipates after May (Figure 2d). On the interannual and interdecadal timescales, the significant periods of NELPVW volume variation are 7 and 20 years.

Based on previous observations and calculations, as the radiative forcing increases, the ocean warming is surface-intensified and decreases with depth, strengthening the upper ocean's stratification and becoming unfavorable for the low PV water formation (Xu et al., 2013). By linear regression analysis, we found that the volume of CMW has a significant decreasing trend, which is marked by the yellow solid line in Figure 6b. There are no significant linear trends of EMW and STMW from 1871 to 2007. However, as global warming intensifies, the newly discovered NELPVW is the only one low PV water mass with a significant

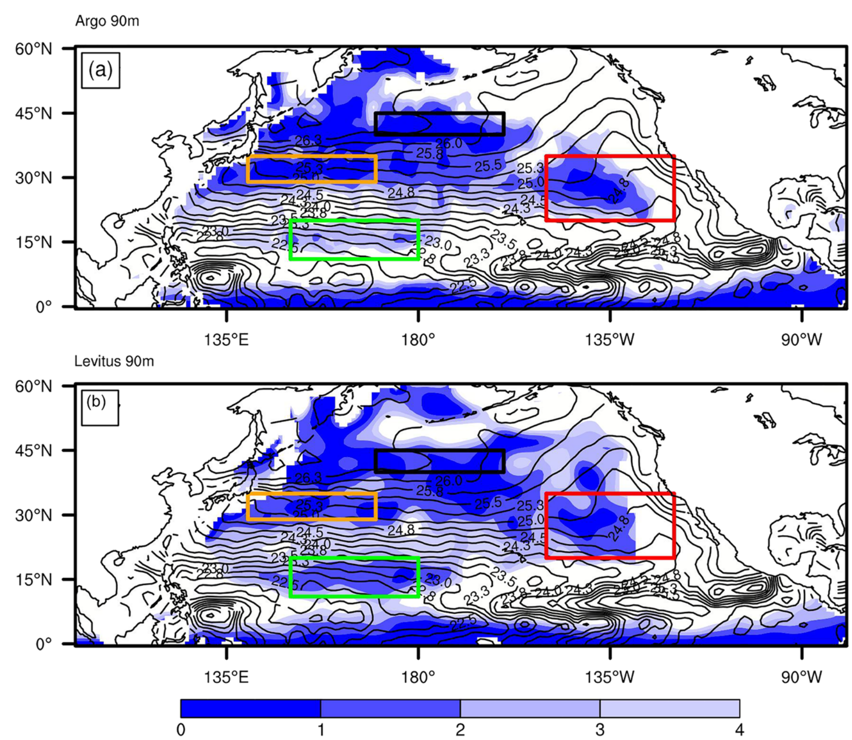

Figure 3. The distribution of long-term mean winter PV (shadings; 10^{-10} m^{-1} s^{-1}) and PD (black contours; kg m^{-3}–1,000) at the depth of 90 m in BOA_Argo data (a) and Levitus-94 data (b) in North Pacific. Green frame represents NELPVW, red frame represents EMW, black frame represents CMW, and orange frame represents STMW.

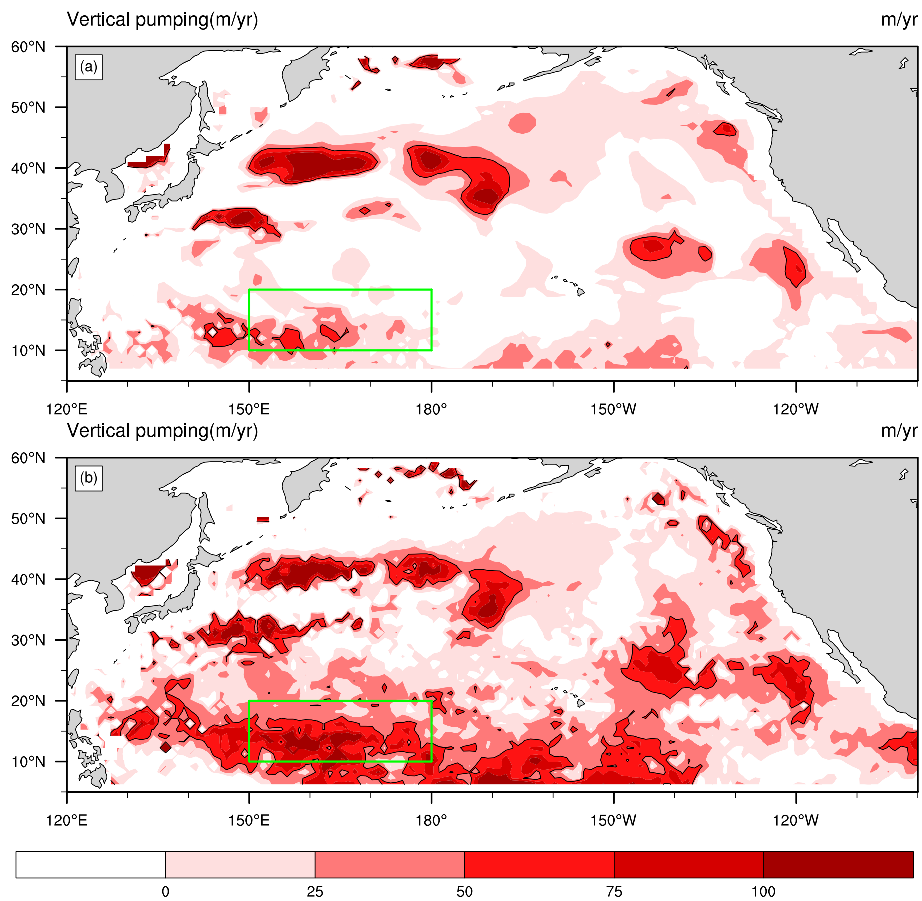

Figure 4. The distributions of long-term mean subduction rate in North Pacific (shadings; m year^{-1}), which are calculated by the Levitus-94 MLD and different flow velocities. (a) Using the geostrophic and Ekman flow velocities calculated by the Levitus data; (b) using SODA 2.2.4 flow velocities. The newly discovered region with a large subduction rate is marked by the green frame.

increasing trend, and the increasing trends of NELPVW subduction rate and the volume of NELPVW are calculated by linear regression analysis and marked by the green solid line and purple solid line in Figure 6d, respectively. This increasing trend may be a kind of modulation of the subsurface ocean to the atmosphere. It seems to us that the long-term NELPVW changes, and its consequences will become increasingly important in the coming decades.

Moreover, the increasing trend of NELPVW subduction rate is largely determined by the change in vertical term (for more details, see Figure S3 in supporting information), which relates to wind stress. NELPVW is shallow and easy to be influenced by atmosphere, and we suspect that the increasing trend may be caused by the change in wind stress. Therefore, we added the regression analysis of regional mean wind stress and MLD in NELPVW generation region. The results of linear regression analysis are shown in supporting information (Figure S4). The absolute values of wind stress components, wind stress curl, and MLD all show significant increasing trends, which proves what we have been guessing before. And the increasing trend of MLD can explain why there is an increasing trend of the lateral induction term of NELPVW subduction rate.

4. The Influence of the North Pacific Low PV Water Masses on the Equatorial Pacific SOT

4.1. Relationship Between North Pacific Low PV Water Masses and SOT in the Equatorial Pacific

After subduction, low PV water mass moves along the isopycnal and diffuses to other regions and affects the dynamic and thermal processes along its trajectory. Therefore, the influence of the North Pacific low PV

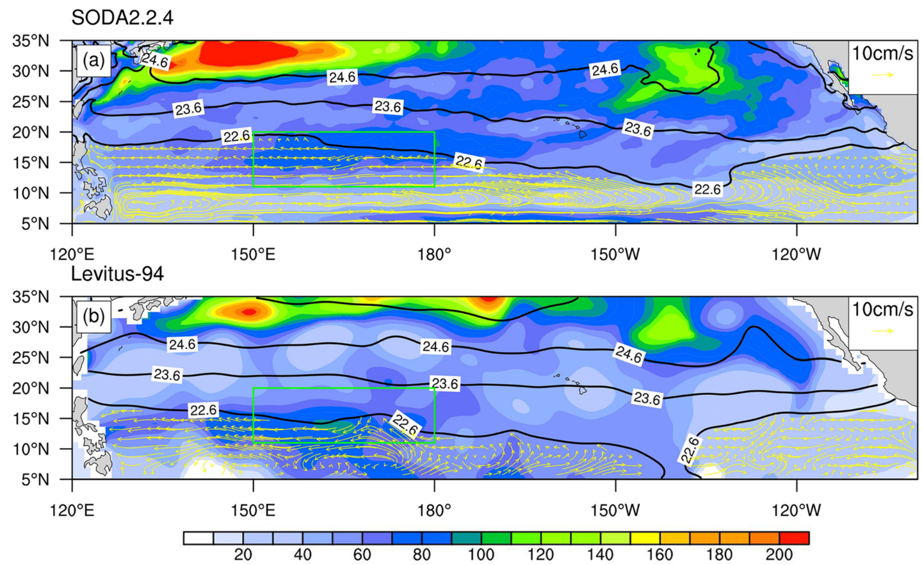

Figure 5. The flow fields among the PD layer of $22.6\sigma_{\theta}$ (vector arrows; cm s^{-1}), MLD (shadings; m) and PD (black contours; kg m^{-3}–1,000) analyzed by different data sets in March. (a) Long-term mean March flow fields, MLD, and PD calculated by SODA 2.2.4; (b) long-term mean March geostrophic and Ekman flow fields, MLD, and PD calculated by Levitus-94 data.

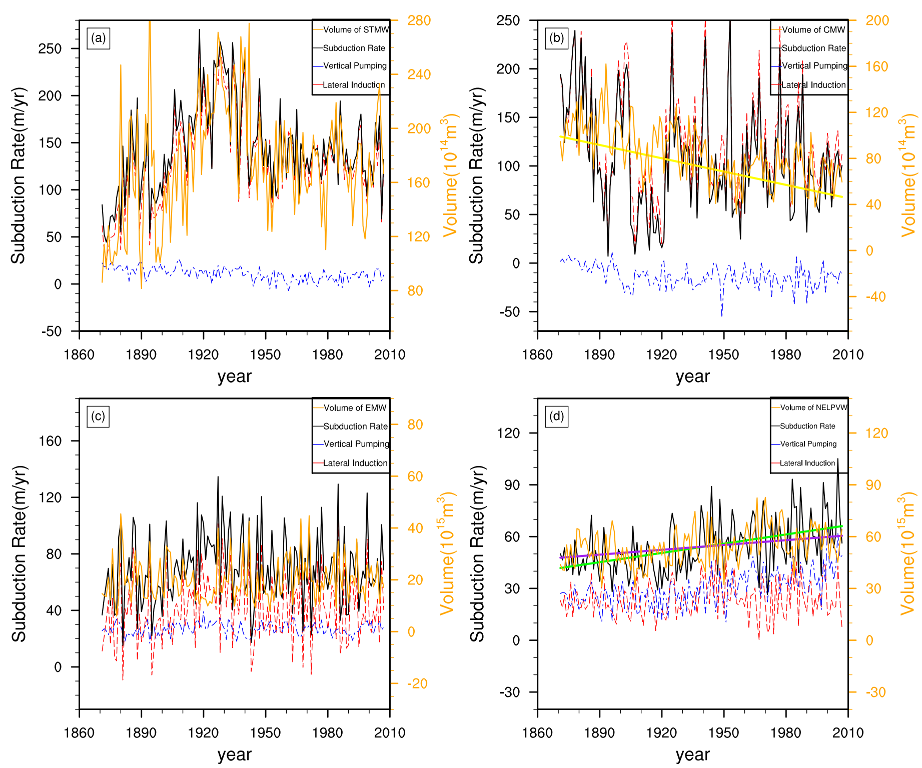

Figure 6. The variation of the low PV water volume (orange solid line; 10^{14} m^3 (10^{15} m^3), a: STMW; b: CMW; c: EMW; d: NELPVW) in the North Pacific, and the corresponding regional mean (the relevant regions are marked in Figure 2b) annual subduction rate (black solid line; m $year^{-1}$), its lateral component (red dashed line; m $year^{-1}$), and vertical component (blue dashed line; m $year^{-1}$). The decreasing trend of CMW volume is marked by the yellow solid line in (b). The increasing trend of NELPVW subduction rate is marked by the green solid line in (d), and the increasing trend of NELPVW volume is marked by the purple solid line in (d). All of these trends pass the 95% significance of *t* test.

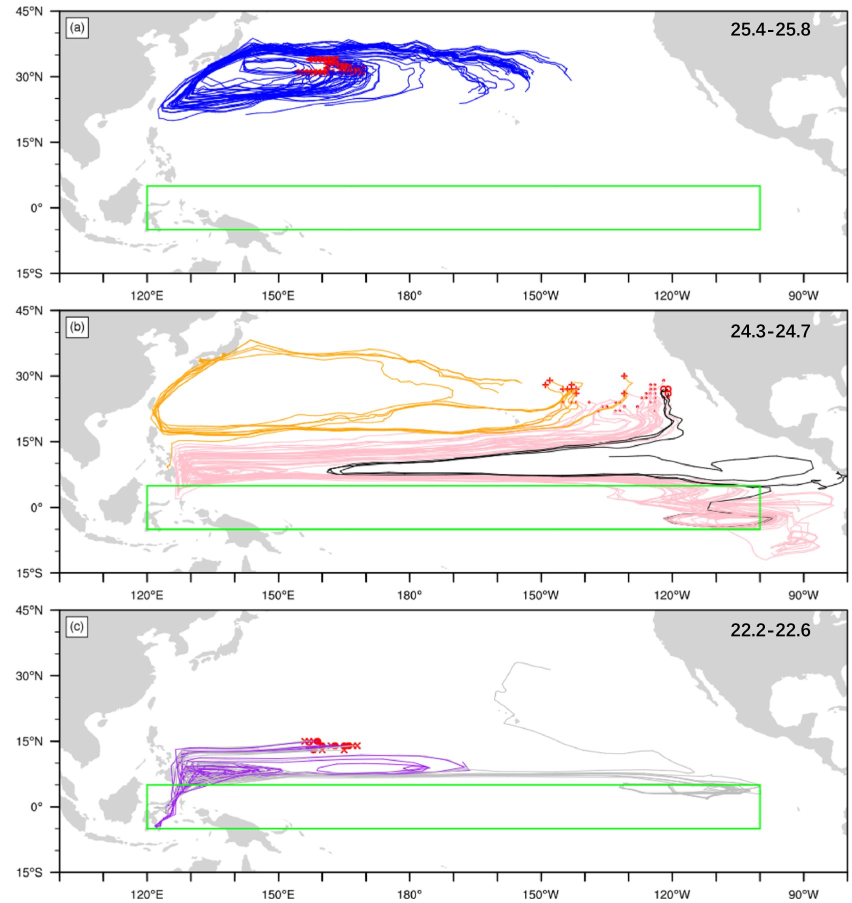

Figure 7. The transport paths of low PV water masses in North Pacific. (a) The transport paths of STMW and CMW among the PD range from 25.4 to 25.8σ_θ; (b) the transport paths of EMW among the PD range from 24.3 to 24.7σ_θ; (c) the transport paths of NELPVW among the PD range from 22.2 to 22.6σ_θ. Red mark represents the starting point; solid line represents the trajectory analyzed by Lagrange-tracking; the tropical region which is affected by low PV water masses in North Pacific is marked by green frame.

water masses on the SOT is a nonlocal process. To influence the equatorial SOT, the low PV water mass must migrate from the source area to the equatorial Pacific by adiabatic motion. To analyze the transport paths of low PV water masses after subduction between low and middle latitudes, Lagrange-tracing of the water particle is carried out at different low PV water mass source areas in the North Pacific.

The transport paths of four low PV water masses in North Pacific are shown in Figure 7. The results show that affected by the Kuroshio, STMW, and CMW can only turn around or reach the subpolar region in the Northwest Pacific but cannot affect the equatorial ocean. However, according to tracing trajectories, it is found that the EMW and NELPVW can affect the equatorial ocean through four transport paths in the subtropical North Pacific. The EMW has two equatorward transport paths, which are called the Western-EMW path and the Central-EMW path, marked by pink solid line and black solid line respectively in Figure 7b. After subduction, a part of EMW is transported through the Western-EMW path and moves southward after reaching the western boundary. Meanwhile, the part transported through the Central-EMW path moves southward to the eastern equatorial Pacific. There are also two paths for the migration of NELPVW. One is the Western-NELPVW path, which represents that the low PV water mass transports to the Indian Ocean through the Malacca Strait along the Mindanao Current, marked by purple solid line in Figure 7c. The other is the Eastern-NELPVW path, which represents that the low PV water mass transports to the Middle East Pacific along the Equatorial Countercurrent, marked by gray solid line in Figure 7c.

10.1029/2020JC016282

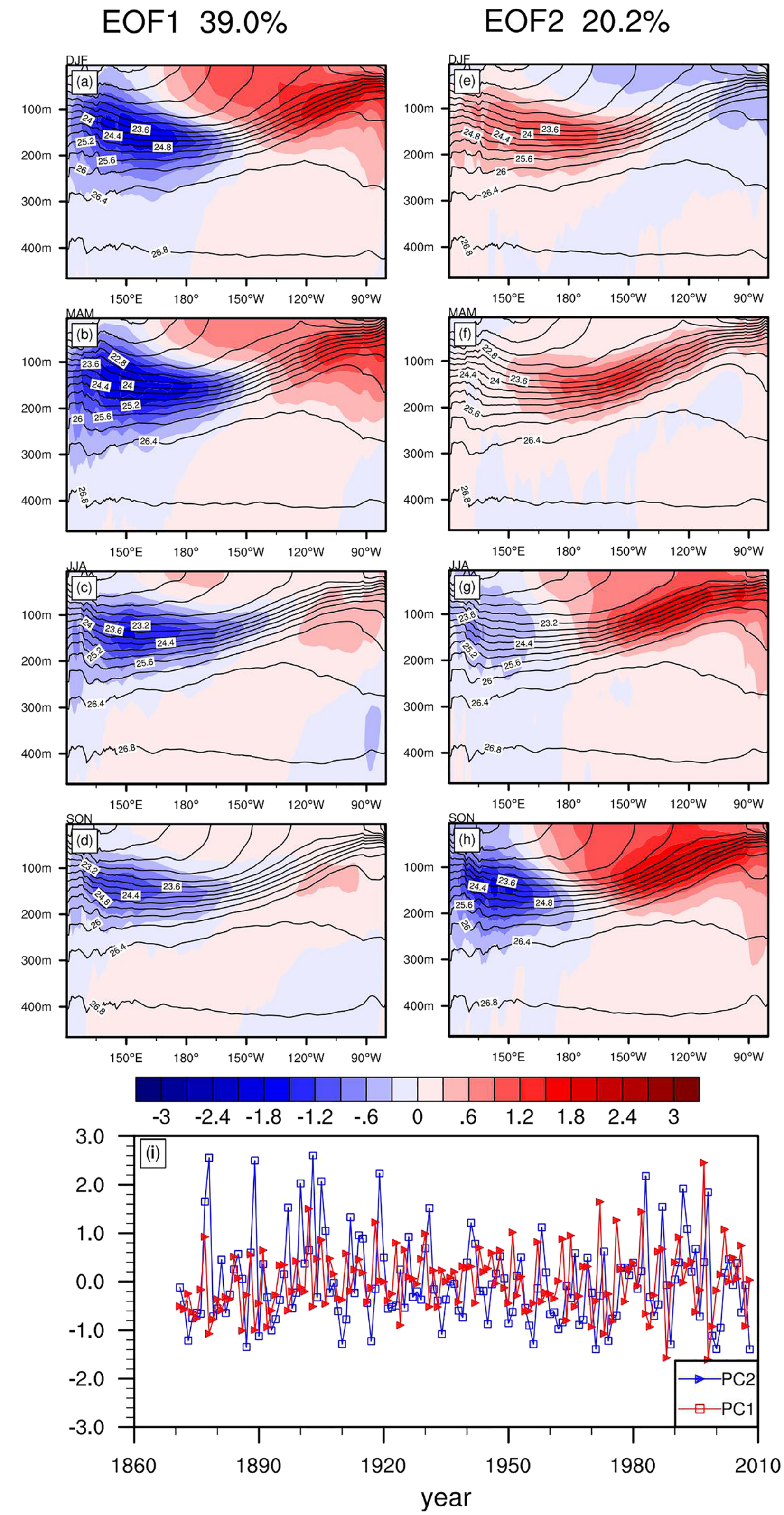

Figure 8. The MV-EOF principal modes and corresponding time series of the equatorial SOT (shadings: °C) and seasonal variations of long-term mean PD (black contours; kg m^{-3}–1,000) from winter to autumn. (a–d) The variation of EOF1 from winter to autumn; (e–h) the variation of EOF2 from winter to autumn; (i) the corresponding time series, the red line represents PC1, and the blue line represents PC2.

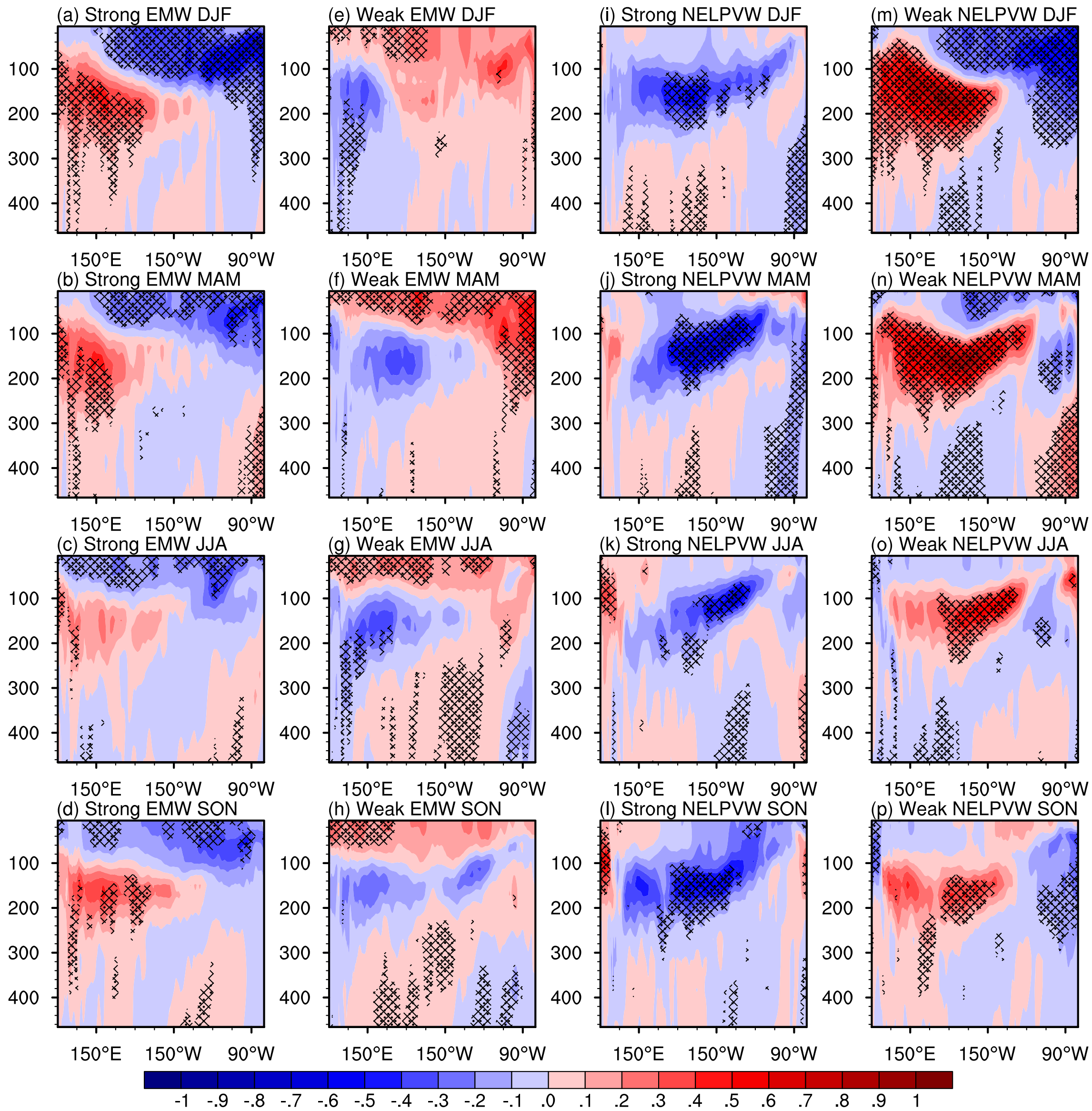

Figure 9. Seasonal synthesis of equatorial SOT anomalies (shadings; °C) in strong (weak) EMW (NELPVW) subduction years. (a–d) In the strong EMW subduction years; (e-h) in the weak EMW subduction years; (i–l) in the strong NELPVW subduction years; (m–p) in the weak NELPVW subduction years. The area that passed the 80% significance of *t* test is covered with crosses, and the area that passed the 85% significance of *t*-test is covered with dots.

Both the Western-EMW path and the Western-NELPVW path can affect the western equatorial Pacific. And both the Central-EMW path and the Eastern-NELPVW path can affect the eastern equatorial Pacific. It is easy to imagine that, through these paths, the two low PV water masses may bring atmospheric forcing signals of the Subtropical North Pacific into the equatorial subsurface layer directly and furthermore affect the atmosphere above equatorial Pacific. It offers a new insight to study the possible mechanisms for the interaction between the subtropical and tropical North Pacific.

In order to verify these hypotheses, we performed a MV-EOF analysis of the equatorial subsurface oceanic temperature (SOT). The result shows that the first two loading vector fields reflect well the whole anomaly pattern structure of SOT in equatorial Pacific (Figure 8). The spatial distributions of the first and second modes are quite different. The first EOF mode accounts for 39.0% of the total variance, the corresponding spatial structure, EOF1, shows abnormally warm in the western equatorial Pacific but abnormally cold in the eastern equatorial Pacific, which is similar to the ENSO-like tropical Pacific decadal variability

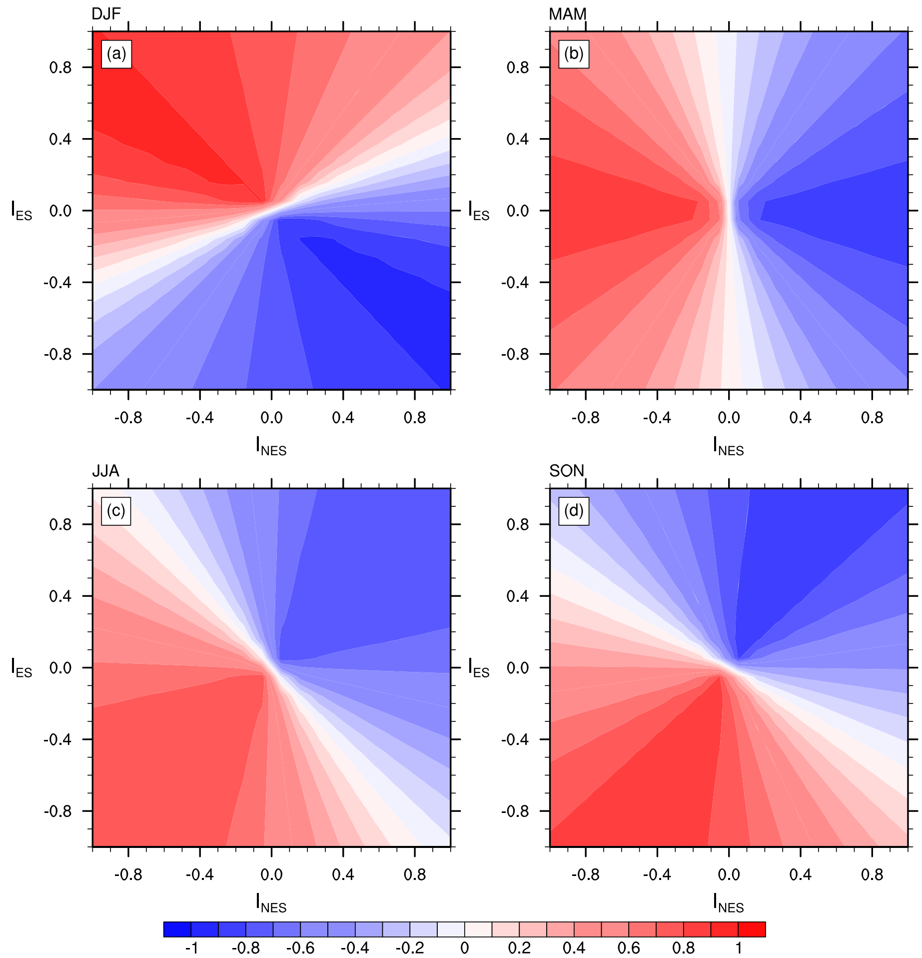

Figure 10. The MV-EOF second mode of equatorial SOT ($SOT_{second\ mode}$) can be represented by the weighted linear combination of the seasonal synthesis of equatorial SOT anomalies in the strong EMW subduction years and the strong NELPVW subduction years (I_{ES}*SOT_{ES} + I_{NES}*SOT_{NES}). The different distributions of spatial correlation coefficients between $SOT_{second\ mode}$ and I_{ES}*SOT_{ES} + I_{NES}*SOT_{NES} in DJF (a), MAM (b), JJA (c), and SON (d) vary with variables I_{ES} (vertical coordinate) and I_{NES} (horizontal coordinate).

proposed by Choi et al. (2013). The temperature anomaly mainly appears among the potential density layers between 23.5 and 25σ_θ, and the depth where the large temperature anomaly appears is deeper in the west but shallower in the east. The second EOF mode accounts for 20.2% of the total variance; the corresponding spatial structure, EOF2, is similar to the ENSO-induced tropical Pacific decadal variability proposed by Choi et al. (2013), especially in spring. Moreover, EOF2 reflects distinct seasonal signals. It is found that the warm anomaly propagates from deep layer in western equatorial Pacific in winter to shallow layer in western equatorial Pacific in autumn.

Furthermore, we have calculated the correlation coefficients between the two low PV water masses' annual subduction rates and the corresponding time series of EOF1 and EOF2. It is found that the annual regional-averaged subduction rate of EMW is significantly negatively correlated with the corresponding time series of EOF1, while the annual regional-averaged subduction rate of NELPVW is positively correlated with the corresponding time series of EOF1 and negatively correlated with the corresponding time series of EOF2; the correlation coefficients are −0.12, 0.16, and −0.17, respectively, and all the correlations passed the 95% significance of *t* test. This indicates that the subduction process over the North Pacific may affect the equatorial SOT. According to the correlation coefficients, with the larger EMW subduction rate, the SOT tends to display warm anomaly in the western equatorial Pacific but cold anomaly at the upper layer in the eastern

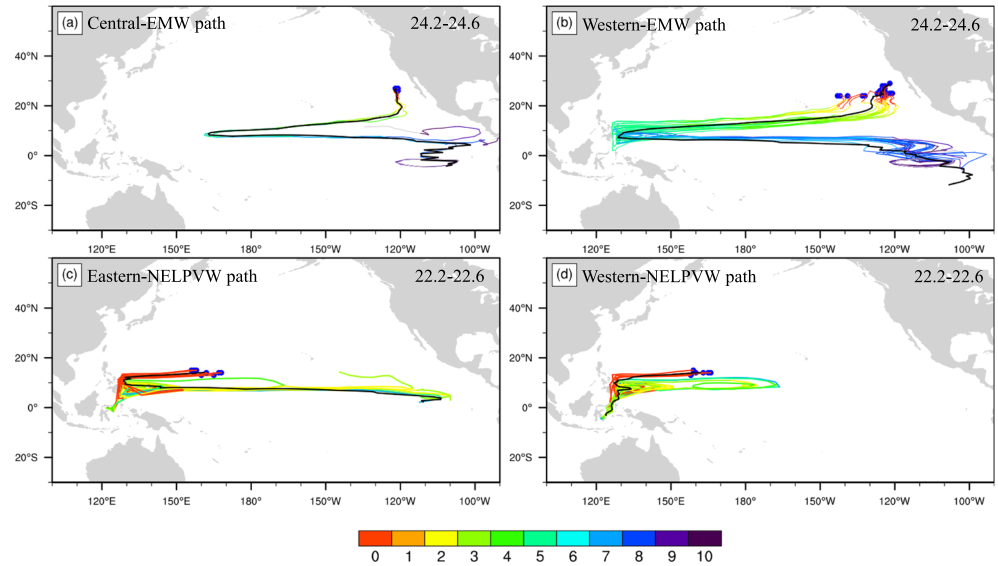

Figure 11. The equatorward-transport paths (solid line) and the corresponding times (shadings; year) of two low PV water masses. (a) The Central-EMW path among the PD ranges from 24.2 to 24.6σ_θ; (b): the Western-EMW path among the PD ranges from 24.2 to 24.6σ_θ; (c) the Eastern-NELPVW path among the PD ranges from 22.2 to 22.6σ_θ; (d) the Western-NELPVW path among the PD ranges from 22.2 to 22.6σ_θ.

equatorial Pacific. However, accompanying with the larger NELPVW subduction rate, the SOT tends to display cold anomaly at the central and warm anomaly at both the eastern and western equatorial Pacific.

The year which annual regional-averaged subduction rate anomaly exceeds the positive (negative) 1.75 standard deviation is defined as extremely strong (weak) subduction year. There are 33 extremely strong subduction years and 32 extremely weak subduction years in the EMW subduction area, 31 extremely strong subduction years, and 33 extremely weak subduction years in the NELPVW subduction area. Based on the method of composite analysis, the seasonal variations of SOT anomaly over equatorial Pacific in strong

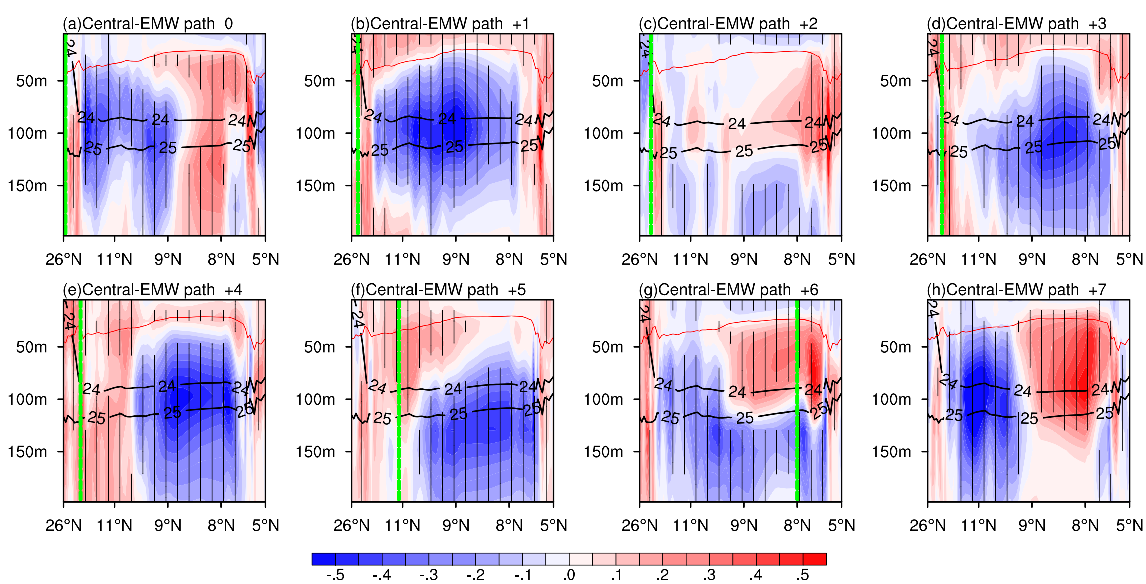

Figure 12. Composed equatorial SOT anomaly (shadings;°C) profiles, PD (black contours; kg m^{-3}–1,000), and MLD (red solid line; m) in the strong EMW subduction years along the Central-EMW path from the year in the occurrence of the subduction to the 7 years later at 1-year intervals. Green solid line represents the latitude where the EMW reaches. The area that passed the 90% significance of *t* test is covered with vertical lines.

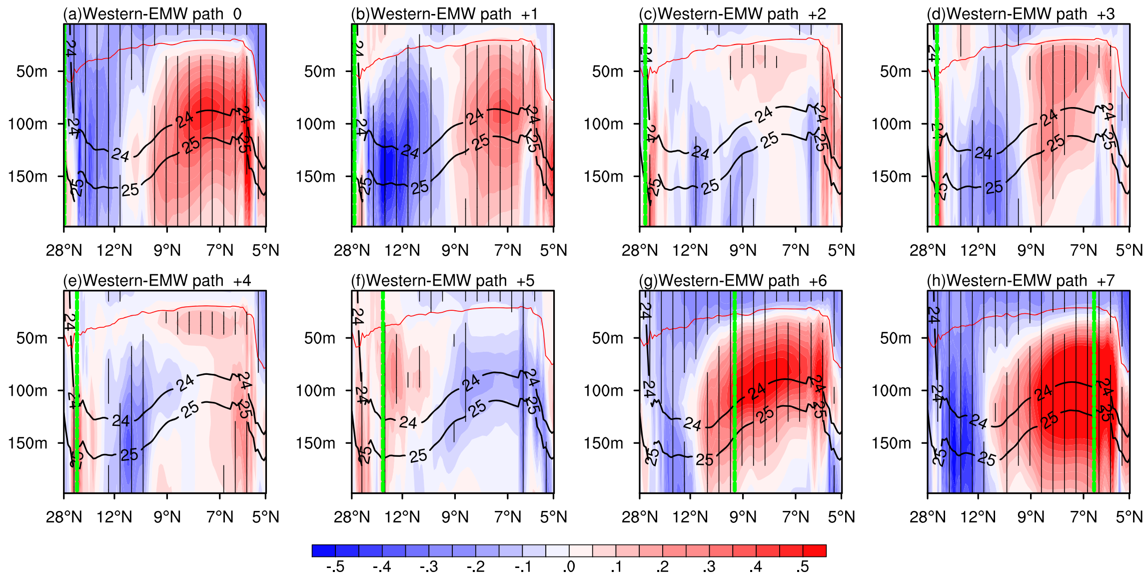

Figure 13. Composed equatorial SOT anomaly (shadings;°C) profiles, PD (black contours; kg/m^{-3}–1,000), and MLD (red solid line; m) in the strong EMW subduction years along the Western-EMW path from the year in the occurrence of the subduction to the 7 years later at 1-year intervals. Green solid line represents the latitude where the EMW reaches. The area that passed the 90% significance of *t* test is covered with vertical lines.

(weak) EMW (NELPVW) subduction years are investigated (Figure 9). The results show that, in the strong EMW subduction years, the SOT anomaly in equatorial Pacific is positive in the east and negative in the west, and the largest positive SOT anomaly appears in the depth range of 100 to 200 m among 120°E–160°W. In the weak EMW subduction years, the SOT anomaly is positive in the west and negative in the east, and the longitude range of the negative SOT anomaly varies with season. SOT anomaly reaches the minimum value at the range of 120°–170°E in winter and gradually extends eastward to the eastern Pacific in the following season. It is worth mentioning that the subduction of low PV water happens every year, and its impact is also continuous. Therefore, we give the equatorial SOT anomalies in 3.5 and 7 years after the strong (weak) EMW subduction years (for more details, see Figures S5 and S6 in supporting information).

The composite SOT anomaly in strong (weak) NELPVW subduction years in near-equatorial region is different from those in the eastern region. In the strong NELPVW subduction years, the SOT of equatorial Pacific is a tripolar structure, which is cold in the center and warm in the east and west. The area with warm anomaly is relatively shallow in the Northwest Pacific near 100°E and the Northeast Pacific near 140°W. The area with cold anomaly is in the center of equatorial Pacific and generally shallower to westward along the thermocline. The SOT in the weak NELPVW subduction years is the complete opposite of that in the extremely strong subduction years, which is a cold-warm-cold structure, stretching farther west compared with the position in winter.

The distribution of SOT anomaly in the strong EMW (NELPVW) subduction years is almost precisely the opposite of that in the weak subduction years, which suggests that the subduction process over the North Pacific plays a great role in the equatorial SOT. Moreover, we noticed that the SOT anomaly spatial distribution in EOF1 and strong (weak) EMW subduction year is very similar, while the SOT anomaly spatial distribution in EOF2 is more complicated. Therefore, we calculated the spatial correlation coefficients between EOF1 (EOF2) and SOT anomaly in strong EMW (NELPVW) subduction year. It is found that EOF1 has the best correlation with the SOT anomaly in strong EMW subduction, and the spatial correlation coefficient is −0.84. EOF2 is correlated well with the strong NELPVW subduction year results, the spatial correlation coefficient is −0.50, and the spatial correlation coefficient is −0.18 between EOF2 and the strong EMW subduction year results. All the correlations passed the 99% significance of *t* test.

In the light of the correlations, the MV-EOF second mode of equatorial SOT (SOT_{EOF2}) can be represented by the weighted linear combination of the synthesis of equatorial sea temperature anomalies in the EMW strong subduction years and the NELPVW strong subduction years (I_{ES}*SOT_{ES} + I_{NES}*SOT_{NES}). The different distribution of spatial correlation coefficient between SOT_{EOF2} and I_{ES}*SOT_{ES} + I_{NES}*SOT_{NES} in each season caused by variables I_{ES} and I_{NES} is shown in Figure 10. When I_{ES} and I_{NES} reach a certain proportion, SOT_{EOF2} and I_{ES}*SOT_{ES} + I_{NES}*SOT_{NES} have the best correlation. And the proportion varies significantly with the seasons, which implies that the effect of two low PV water masses on equatorial sea subsurface temperature has obvious seasonal difference. In winter, to reach the best correlation, the proportion of SOT_{NES} should be slightly larger than SOT_{ES}. While in spring, the effect of NELPVW on equatorial sea subsurface temperature seems to predominate. The possible reasons are that the subduction processes of EMW and NELPVW both begin in winter, and the volume of two low PV water masses increase and both reach the peak in April (Figure 2d), and considering the distance between the regions of two low PV water masses and equatorial Pacific, it takes a while for EMW to reach the equatorial Pacific after subduction; therefore the impact of NELPVW subduction process on equatorial SOT is primary in spring. In summer, to reach the best correlation, the SOT_{ES} to SOT_{NES} radio should be nearly one to one. And in autumn, the proportion of SOT_{ES} should be slightly larger than SOT_{NES}. It suggests that the effect of EMW on equatorial SOT is growing. Since the depth range of NELPVW is the shallowest, it is much easier to influence by atmosphere, and the temperature anomaly may be more difficult to retain and influence on the equatorial SOT further.

4.2. The Mechanism of the EMW and NELPVW Effecting on the Equatorial Pacific SOT

The transport path and time of low PV water mass can be obtained by Lagrange tracking method (Figure 11). EMW, which generates in the subtropical Northeast Pacific, can migrate and bring SOT anomaly to the equatorial Pacific along the Central-EMW and Western-EMW paths and has a further impact on the eastern and the western equatorial Pacific, respectively. Unlike the EMW, NELPVW can migrate to the Indian Ocean through the Malacca Strait along with the Mindanao Current by the Western-NELPVW path or migrate to the Middle East Pacific along the Equatorial Countercurrent by the Eastern-NELPVW path. The different characteristics of different low PV water masses will no doubt have various impacts on the equatorial Pacific. It is found that two equatorward-transport paths of EMW (Central-EMW and Western-EMW paths) both take less than 7 years to reach the equatorial Pacific. While because of the shorter distance between the NELPVW generation region and the equatorial Pacific, the two equatorward-transport paths of NELPVW (Western-NELPVW and Eastern-NELPVW paths) only take less than 3 years.

Overall, these findings provide support for further investigation of the lag response that the sea temperature anomalies carrying by EMW and NELPVW reach the equatorial Pacific and then affect the equatorial SOT there. And it can be expected that the different transportation times and destinations of the two low PV water masses will lead to more diverse coupling results of SOT in equatorial Pacific. To verify this, temperature profiles in the strong EMW subduction years are synthesized along the two transport paths of EMW from the year in the occurrence of the subduction to the 7 years later at 1-year intervals. It is found that in strong EMW subduction years, positive temperature anomaly travels from about 26°N in the EMW source region to the equatorial Pacific along Central-EMW path (Figure 12), and in the meantime, another positive temperature anomaly travels from about 28°N in the EMW source region to about 6°N along Western-EMW path (Figure 13). The combined effect of the two equatorward-transport paths of EMW makes the distribution of equatorial SOT anomalies display warm in the east but cold in the west.

Differently, the transportation times of two paths of NELPVW are rather shorter, and their influences on the SOT are quite limited. The temperature profiles in the strong NELPVW subduction years along the two transport paths of NELPVW are synthesized too, but we can hardly find the significant temperature anomaly signal companying with the migration paths of NELPVW. One explanation could be that the depth range of NELPVW is the shallowest of the four low PV water in North Pacific, which much easier to influence by atmosphere, and the temperature anomaly may be more difficult to retain and influence on the equatorial SOT further.

5. Summary and Discussion

Using SODA2.2.4 ocean reanalysis data to analyze the subduction rate in the North Pacific, new spatial characteristics of the subduction rate are found. Besides the three main subduction regions in North Pacific, the near-equatorial Pacific region (11–20°N, 145°E–180°) with a high subduction rate is found, which has never been discussed in the previous studies. In this newly discovered high subduction rate area, we find a new low PV water mass, which is named as the near-equator low PV water mass (NELPVW).

The NELPVW is characterized by low PV and nearly vertically homogeneous temperature and salinity distributions. The core PD of NELPVW is less than $23\sigma_\theta$, and the temperature ranges from 20 to 25°C, which is the lightest and warmest of the four low PV water in North Pacific. NELPVW exists in the depth range of 50–120 m, with a flatter three-dimensional structure, which is the shallowest of the four low PV water in North Pacific. Therefore, it is much easier to influence by atmosphere. Moreover, as global warming intensifies, NELPVW is the only one low PV water mass in North Pacific that appears an increasing trend, which means that NELPVW may play a greater role in the subsurface ocean in the future.

Among all the low PV water masses in North Pacific, only EMW and NELPVW can migrate to the equatorial Pacific and effect SOT there. The equatorward-transport paths of EMW and NELPVW and consequent impacts on the equatorial SOT are revealed. In the strong EMW subduction years, the SOT anomaly in equatorial Pacific is positive in the east and negative in the west. In the strong NELPVW subduction years, the SOT anomaly of equatorial Pacific is negative in the center and positive in the east and west. The equatorial SOT anomaly in the strong NELPVW (EMW) subduction years is completely opposite to those weak subduction years.

MV-EOF analysis of the equatorial SOT shows that the first two loading vector fields reflect well the whole anomaly pattern structure of SOT in equatorial Pacific. EOF1 shows abnormally warm in the western equatorial Pacific but abnormally cold in the eastern equatorial Pacific, which accounts for 39.0% of the total variance. EOF2 accounts for 20.2% of the total variance, which reflect distinct seasonal signals, and the warm anomaly propagates from deep layer in western equatorial Pacific in winter to shallow layer in western equatorial Pacific in autumn. It is found that EOF1 has the best correlation with the SOT anomaly in strong EMW subduction, and the spatial correlation coefficient is −0.84. EOF2 is correlated well with the strong NELPVW subduction year results, the spatial correlation coefficient is −0.50, and the spatial correlation coefficient is −0.18 between EOF2 and the strong EMW subduction year results. All the correlations passed the 99% significance of *t* test. The EOF2 of equatorial SOT can be represented by the weighted linear combination of the synthesis of equatorial SOT anomalies in the EMW strong subduction years and the NELPVW strong subduction years.

Further research shows that the two equatorward-transport paths of EMW both take less than 7 years to reach the equatorial Pacific. While the two equatorward-transport paths of NELPVW only take less than 3 years. In strong EMW subduction years, EMW moves along the two equatorward-transport paths with the positive anomalies of SOT. The combined effect of the two equatorward-transport paths of EMW makes the distribution of equatorial SOT anomalies display warm in the east but cold in the west. However, there is no significant temperature anomaly signal accompanying with the migration paths of NELPVW. One possible reason is that NELPVW is the shallowest of the four low PV water in North Pacific, which is much easier to influence by atmosphere, and the temperature anomaly may be more difficult to retain and influence on the equatorial SOT further.

Data Availability Statement

The SODA reanalysis data used in this study were obtained online (http://apdrc.soest.hawaii.edu/datadoc/soda_2.2.4.php). The BOA_Argo data used in this study were obtained online (ftp://data.argo.org.cn/pub/ARGO/BOA_Argo/). The Levitus-94 monthly data used in this study were obtained online (http://iridl.ldeo.columbia.edu/SOURCES/.LEVITUS94/.MONTHLY/.

Acknowledgments
ZhiBin Wen and Ziyi Wang contribute equally as first authors. This work has benefited from the discussions with William Perrie of BIO. The revision of manuscript has benefited from the suggestions by Xiaopei Lin and Baolan Wu of OUC. This work was supported by the National Key Program for Developing Basic Science (grants 2016YFA0600303 and 2018YFC1505900), the National Natural Science Foundation of China (grants 41330420, 41621005, 41675064, 41675067, and 41875086), the Jiangsu Province Science Foundation (grant no. BK2020020170). The authors are thankful for the support from the Jiangsu Provincial Innovation Center for Climate Change and Fundamental Research Funds for the Central University. This work was jointly supported by the Joint Open Project of KLME and CIC-FEMD (grant KLME201902).

References

Carton, J. A., Giese, B. S., & Grodsky, S. A. (2005). Sea level rise and the warming of the oceans in the Simple Ocean Data Assimilation (SODA) ocean reanalysis. *Journal of Geophysical Research*, *110*, C09006. https://doi.org/10.1029/2004JC002817

Chen, J., Qu, T., Sasaki, Y. N., & Schneider, N. (2010). Anti-correlated variability in subduction rate of the western and eastern North Pacific oceans identified by an eddy-resolving ocean GCM. *Geophysical Research Letters*, *37*, L23608. https://doi.org/10.1029/2010GL045239

Choi, J., An, S. I., Kug, J. S., & Yeh, S. W. (2011). The role of mean state on changes in el nino's flavor. *Climate Dynamics*, *37*(5–6), 1205–1215. https://doi.org/10.1007/s00382-010-0912-1

Choi, J., An, S. I., Yeh, S. W., & Yu, J. Y. (2013). ENSO-like and ENSO-induced tropical pacific decadal variability in cgcms. *Journal of Climate*, *26*(5), 1485–1501. https://doi.org/10.1175/jcli-d-12-00118.1

Gu, D., & Philander, S. G. (1997). Interdecadal climate fluctuations that depend on exchanges between the tropics and extratropics. *Science*, *275*(5301), 805–807. https://doi.org/10.1126/science.275.5301.805

Guo, Y., Lin, X., Wei, M., Liu, C., & Men, G. (2018). Decadal variability of North Pacific eastern subtropical mode water. *Journal of Geophysical Research: Oceans*, *123*, 6189–6206. https://doi.org/10.1029/2018JC013890

Hanawa, K. (1987). Interannual variations of the winter-time outcrop area of subtropical low PV water mass in the western North Pacific Ocean. *Atmosphere-Ocean*, *25*(4), 358–374. https://doi.org/10.1080/07055900.1987.9649280

Hanawa, K., & Talley, L. D. (2001). Chapter 5.4 low PV water masss. *International Geophysics*, *77*(01), 373–386. https://doi.org/10.1016/S0074-6142(01)80129-7

Hautala, S. L., & Roemmich, D. H. (1998). Subtropical low PV water mass in the Northeast Pacific Basin. *Journal of Geophysical Research*, *103*(C6), 13,055–13,066. https://doi.org/10.1029/98JC01015

Hu, H., Liu, Q., & Liu, W. (2006). Interannual variation and mechanism of subduction rate in the North Pacific subtropical mode water forming regions (in Chinese with English abstract). *Acta Oceanologica Sinica*, *28*, 22–28. https://doi.org/10.3321/j.issn:0253-4193.2006.02.0

Huang, R. X., & Qiu, B. (1994). Three-dimensional structure of the wind-driven circulation in the subtropical North Pacific. *Journal of Physical Oceanography*, *24*(7), 1608–1622. https://doi.org/10.1175/1520-0485(1994)024<1608:tdSOTw>2.0.co;2

Iselin, C. O. D. (1939). The influence of vertical and lateral turbulence on the characteristics of the waters at mid-depths. *Eos, Transactions American Geophysical Union*, *20*(3), 414–417. https://doi.org/10.1029/TR020i003p00414

Kobashi, F., Mitsudera, H., & Xie, S. P. (2006). Three subtropical fronts in the North Pacific: Observational evidence for low PV water mass-induced subsurface frontogenesis. *Journal of Geophysical Research*, *111*, C09033. https://doi.org/10.1029/2006jc003479

Kubokawa, A., & Xie, S. P. (2002). Steady response of a ventilated thermocline to enhanced ekman pumping. *Journal of Oceanography*, *58*(4), 565–575. https://doi.org/10.1023/A:1021266810832

Lee, H. C. (2009). Impact of atmospheric CO_2 doubling on the North Pacific subtropical mode water. *Geophysical Research Letters*, *36*, L06602. https://doi.org/10.1029/2008GL037075

Levitus, S., & Boyer, T. P. (1994). World ocean atlas 1994. volume 4. temperature. National environmental satellite, data, and information service (No. PB-95-270112/XAB; NESDIS-4), Washington, DC (United States).

Liu, L. L., & Huang, R. X. (2012). The global subduction/obduction rates: Their interannual and decadal variability. *Journal of Climate*, *25*(4), 1096–1115. https://doi.org/10.1175/2011JCLI4228.1

Liu, Q., & Hu, H. (2007). A subsurface pathway for low potential vorticity transport from the central North Pacific toward Taiwan island. *Geophysical Research Letters*, *34*, L12710. https://doi.org/10.1029/2007GL029510

Lu, S. S., Liu, Z. H., Li, H, Li, Z. Q., Wu, X. F., Sun, C. H., & Xu, J. P. (2020). Manual of Global Ocean Argo gridded data set (BOA_Argo) (Version2020), 15 pp.

Luo, Y., Liu, Q., & Rothstein, L. M. (2009). Simulated response of North Pacific mode waters to global warming. *Geophysical Research Letters*, *36*, L23609. https://doi.org/10.1029/2009GL040906

Marshall, J. C., Williams, R. G., & Nurser, A. G. (1993). Inferring the subduction rate and period over the North Atlantic. *Journal of Physical Oceanography*, *23*(7), 1315–1329. https://doi.org/10.1175/1520-0485(1993)023%3C1315:ITSRAP%3E2.0.CO;2

Masuzawa, J. (1969). Subtropical low PV water mass. In. *Deep Sea Research and Oceanographic Abstracts*, *16*(5), 463–472). Elsevier. https://doi.org/10.1016/0011-7471(69)90034-5

McCartney, M. S., & Talley, L. D. (1982). The subpolar low PV water mass of the North Atlantic Ocean. *Journal of Physical Oceanography*, *12*(11), 1169–1188. https://doi.org/10.1175/1520-0485(1982)012%3C1169:TSMWOT%3E2.0.CO;2

McPhaden, M. J., Lee, T., & Mcclurg, D. (2011). El Niño and its relationship to changing background conditions in the tropical Pacific Ocean. *Geophysical Research Letters*, *38*, L15709. https://doi.org/10.1029/2011GL048275

McPhaden, M. J., & Zhang, D. (2002). Slowdown of the meridional overturning circulation in the upper Pacific Ocean. *Nature*, *415*(6872), 603–608. https://doi.org/10.1038/415603a

Nakamura, H. (1996). A pycnostad on the bottom of the ventilated portion in the central subtropical North Pacific: Its distribution and formation. *Journal of Oceanography*, *52*(2), 171–188. https://doi.org/10.1007/BF02235668

Oka, E., Kouketsu, S., Toyama, K., Uehara, K., Kobayashi, T., Hosoda, S., & Suga, T. (2011). Formation and subduction of central low PV water mass based on profiling float data, 2003–08. *Journal of Physical Oceanography*, *41*(1), 113–129. https://doi.org/10.1175/2010jpo4419.1

Qiu, B., & Huang, R. X. (1995). Ventilation of the North Atlantic and North Pacific: Subduction versus obduction. *Journal of Physical Oceanography*, *25*(10), 2374–2390. https://doi.org/10.1175/1520-0485(1995)0252.0.CO;2

Qu, T., & Chen, J. (2009). A North Pacific decadal variability in subduction rate. *Geophysical Research Letters*, *36*, L22602. https://doi.org/10.1029/2009GL040914

Shi, F., Luo, Y., & Xu, L. (2018). Volume and transport of eddy-trapped mode water south of the Kuroshio extension. *Journal of Geophysical Research: Oceans*, *123*, 8749–8761. https://doi.org/10.1029/2018JC014176

Stommel, H. (1979). Determination of water mass properties of water pumped down from the Ekman layer to the geostrophic flow below. *Proceedings of the National Academy of Sciences*, *76*(7), 3051–3055. https://doi.org/10.2307/69926

Suga, T., Takei, Y., & Hanawa, K. (1997). Thermostad distribution in the North Pacific subtropical gyre: The central low PV water mass and the subtropical low PV water mass. *Journal of Physical Oceanography*, *27*(1), 140–152. https://doi.org/10.1175/1520-0485(1997)027<0140:tditnp>2.0.co;2

Sugimoto, S., Hanawa, K., Watanabe, T., Suga, T., & Xie, S. P. (2017). Enhanced warming of the subtropical low PV water mass in the North Pacific and North Atlantic. *Nature Climate Change*, *7*(9), 656–658. https://doi.org/10.1038/nclimate3371

Toyama, K., Iwasaki, A., & Suga, T. (2015). Interannual variation of annual subduction rate in the North Pacific estimated from a gridded Argo product. *Journal of Physical Oceanography*, *45*(9), 2276–2293. https://doi.org/10.1175/JPO-D-14-0223.1

Wang, B. (2010). The vertical structure and development of the enso anomaly mode during 1979–1989. *Journal of Atmospheric Sciences*, *49*(8), 698–712. https://doi.org/10.1175/1520-0469(1992)049%3C0698:TVSADO%3E2.0.CO;2

Wen, Z., Hu, H., Song, Z., Bai, H., & Wang, Z. (2020). Different influences of mesoscale oceanic eddies on the North Pacific subsurface low potential vorticity water mass between winter and summer. *Journal of Geophysical Research: Oceans*, *125*, e2019JC015333. https://doi.org/10.1029/2019JC015333

Worthington, L. V. (1959). The 18° water in the sargasso sea. *Deep Sea Research*, *5*(2), 297–305. https://doi.org/10.1016/0146-6313(58)90026-1

Wu, B., Lin, X., & Yu, L. (2020). North Pacific subtropical mode water is controlled by the Atlantic multidecadal variability. *Nature Climate Change*, *10*(3), 238–243. https://doi.org/10.1038/s41558-020-0692-5

Xu, L., Xie, S. P., & Liu, Q. (2013). Fast and slow responses of the North Pacific mode water and subtropical countercurrent to global warming[J]. *Journal of Ocean University of China*, *12*(2), 216–221. https://doi.org/10.1007/s11802-013-2189-6

Yasuda, T., & Hanawa, K. (1997). Decadal changes in the low PV water masss in the midlatitude North Pacific. *Journal of Physical Oceanography*, *27*(6), 858–870. https://doi.org/10.1175/1520-0485(1997)027<0858:DCITMW>2.0.CO;2

Yu, K., Qu, T., Dong, C., & Yan, Y. (2015). Effect of subtropical mode water on the decadal variability of the subsurface transport through the Luzon Strait in the western Pacific Ocean. *Journal of Geophysical Research: Oceans*, *120*, 6829–6842. https://doi.org/10.1002/2015JC011016